JOURNAL OF SPACECRAFT AND ROCKETS
Vol. 43, No. 3, May–June 2006

Electron Flux Formations at Middle Latitudes in the Surface Dose of Spacecraft

O. R. Grigoryan,* V. N. Sheveleva,† L. S. Novikov,‡ and V. L. Petrov§
Lomonosov Moscow State University, 119899, Moscow, Russia
K. Kudela¶
Slovak Academy of Science, 04353, Kosice, Slovakia
and
I. V. Tchurilo**
Rocket Space Corporation "Energia," 141070, Korolyev, Russia

In this work experimental data on electron fluxes with energies of 30–500 keV obtained from the ACTIVE satellite experiment (INTERCOSMOS-24 in 1989–1990, altitude from 500 km up to 2500 km) and ones with energies 0.3–1.0 MeV obtained onboard the MIR station (SPRUT-VI experiment in 1999, altitude from 350 km up to 400 km) are presented. The distribution of electron fluxes at low and middle latitudes and the influence of charged particles on surface layers of materials and film coverings are investigated. The comparison with results of other satellite experiments reveals the time and spatial stability of electron flux enhancements at $L = 1.2$–1.8.

Nomenclature

E_e = energy range for electrons
E_p = energy range for protons
H = altitude of the satellite above the Earth
I = orbit inclination
L = so-called L-shell parameter ($L = r_{\text{equator}}/R_{\text{Earth}}$)

I. Introduction

IN the present study we analyze the influence of low-energy charged particles (mostly electrons with energy up to 1 MeV) on surface layers of materials and on film coverings. These particles are regularly registered in the inner radiation belt of the Earth by different spacecraft. We analyze electron flux data obtained from the ACTIVE (INTERCOSMOS-24) satellite experiment ($E_e < 500$ keV, orbit altitude $H = 500$–2500 km, orbit inclination $I = 81$ deg), the SPRUT-VI experiment onboard the MIR station ($E_e = 0.3$–1.0 MeV, orbit altitude $H = 350$ km, orbit inclination $I = 51.6$ deg), and the SAMPEX satellite experiment ($E_e > 150$ keV, orbit altitude $H = 520$–670 km, orbit inclination $I = 82$ deg). These electrons were measured at geomagnetic index $L < 2$. The electron flux data were used for calculation of surface dose (thickness of layer of materials up to 10–20 μm) and the distributions of surface dose and electron spectra were constructed for altitudes 500–1500 km. The authors's results were compared with results of calculations based on the average electron flux distribution (AE8) model. It is concluded that the contribution of middle-latitude formations unaccounted for in previous models is insignificant at low altitudes (<600 km) (Ref. 1).

II. Instrumentation

In this paper a detailed analysis of electron flux data obtained onboard the ACTIVE (INTERCOSMOS-24) satellite is presented. Electrons were registered with single Si surface barrier detectors. The diameter and width of each detector were 8 mm and 300 μm correspondingly. The geometric factor of electron detectors was 0.03 cm^2 sr. Three pairs of detectors measured electron fluxes at different angles (99, 69, and 39 deg) with respect to the zenith axis of the satellite. All detectors were protected by Mylar® foil to stop protons with energy $E_p < 500$ keV. The period between subsequent electron flux measurements was 10 s. The peculiarities of the satellite orbit allowed analysis of electron distribution in a wide range of altitudes. The ACTIVE satellite was launched into a 500×2500 km orbit with an inclination of 81 deg. The detectors of the ACTIVE investigation measured electrons in seven energy channels from 30 to 500 keV.

The detectors did measure just electrons with energies of tens and hundreds of MeV. This could be concluded from the two following figures. Figure 1 shows the probability of electron energy absorption depending on the thickness of absorbent. The dashed line marks the thickness of detectors used in the ACTIVE experiments. It is obvious from Fig. 1 that for electrons with energies up to 250 keV (i.e., for energy channels 1–6, excluding the last, highest energy channel) the effectiveness of electron registration comes to 90%.

High-energy protons do not contribute the measured electron fluxes at selected areas. It is seen from Fig. 2 that high-energy proton counts are negligible (<10 particles per second) in comparison with electron counts (200–300 particles per second) (Ref. 2).

III. Observations

Electron fluxes in the inner radiation belt have been observed in different experiments since the 1980s (see Fig. 3). Previous experiments revealed the existence of electrons at $L = 1.2$–1.8 (Ref. 3).

Comparison of the mentioned experiments shows that locations of observed electron precipitation zones are similar. These zones have temporal and spatial stability.

Examples of electron flux registration in the SAMPEX campaign at different L values are presented in Fig. 4. The existence of electron flux enhancements at $L = 1.2$–1.8 is obvious from Fig. 4. We see a broad weak peak around $L = 1.3$, a relatively narrower peak near $L = 1.7$, and another narrow peak near $L = 2.5$. Here is clear

Presented as Paper 2004-2 at the 7th International Conference on Protection of Materials and Structures from Space Environment, Toronto, ON, Canada, 10–13 May 2004; received 25 January 2005; revision received 28 September 2005; accepted for publication 3 October 2005.

*Head of Laboratory, Department of Space Physics Research, Skobeltsyn Institute of Nuclear Physics, Vorobyevy Gory; orsri@srd.sinp.msu.ru.

†Ph.D. Student, Department of Space Physics Research, Skobeltsyn Institute of Nuclear Physics, Vorobyevy Gory.

‡Head of Department, Department of Space and Nuclear Research, Skobeltsyn Institute of Nuclear Physics, Vorobyevy Gory.

§Student, Department of Space Physics Research, Skobeltsyn Institute of Nuclear Physics, Vorobyevy Gory.

¶Head of Laboratory, Institute of Experimental Physics.

**Deputy Chief of Rocket Space Department, 4a Lenina Street.

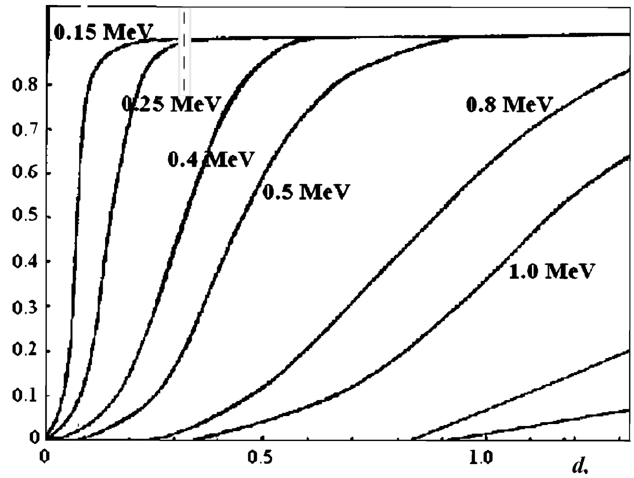

Fig. 1 Probability of electron registration with a single Si-surface barrier detector depending on electron energies and thickness of absorbent.

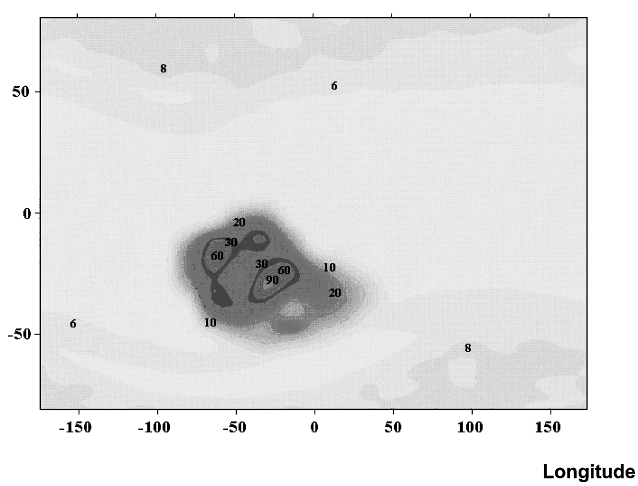

Fig. 2 Proton flux intensities for protons with energies 30–65 MeV observed on board CORONAS-I satellite (altitude 500 km).

evidence that multiple areas of localized precipitation persisted for at least tens of minutes.[4]

The narrow peak could be produced by electron interaction with the lightning-generated waves as they first cross the magnetic equatorial plane (at relatively low L) and before they are reflected. The differences would be due to the latitude of the lightning, to the density gradients in the ionosphere, and to the dependence of precipitation flux on L value.

IV. ACTIVE Experimental Data

The time history of the electron intensity for each energy channel on the ACTIVE satellite is presented in Fig. 5. Two electron enhancements in the L region from 1.2 to 1.8 with maximo at $L = 1.5$ are observed.

The next conclusions follow from the observation of experimental data processing: the longitudinal borders and shape of electron flux registration are stable in time and space for the different year experiments. This proves the existence of a constantly operating mechanism. Electrons are registered at low and middle latitudes at $L = 1.2$–1.8 with maximum intensities at L values approximately 1.3–1.4 and 1.7–1.8.

The next step was the investigation of electron flux distribution as a function of altitude. The wide altitude range allowed comparing zones of electron registration and electron spectra at different altitudes.

Electron flux distribution in geographical coordinates at $L = 1.2$–1.8 for different altitudes is presented on Fig. 6. These maps were constructed using ACTIVE satellite data. Not taking into account all

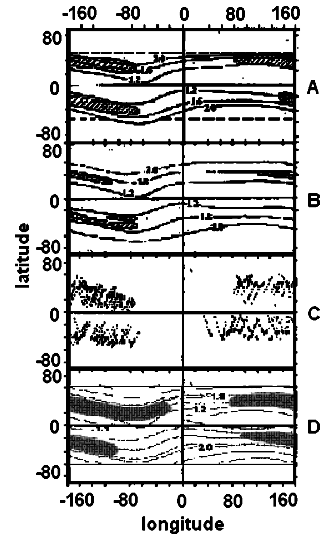

Fig. 3 Areas of registration of the increased electron fluxes at $L < 2$ observed in the following experiments: a) SPRUT-VI experiment on board MIR station, altitude $H = 350$ km, electron energy $E_e > 75$ keV; b) CORONAS-I satellite experiment, altitude $H = 500$ km, electron energy $E_e > 0.5$ MeV; c) OHZORA satellite experiment, altitude $H = 350$–850 km, electron energy $E_e = 0.19$–3.2 MeV; and d) ACTIVE satellite experiment, altitude $H = 500$–2500 km, electron energy $E_e = 30$–500 keV.

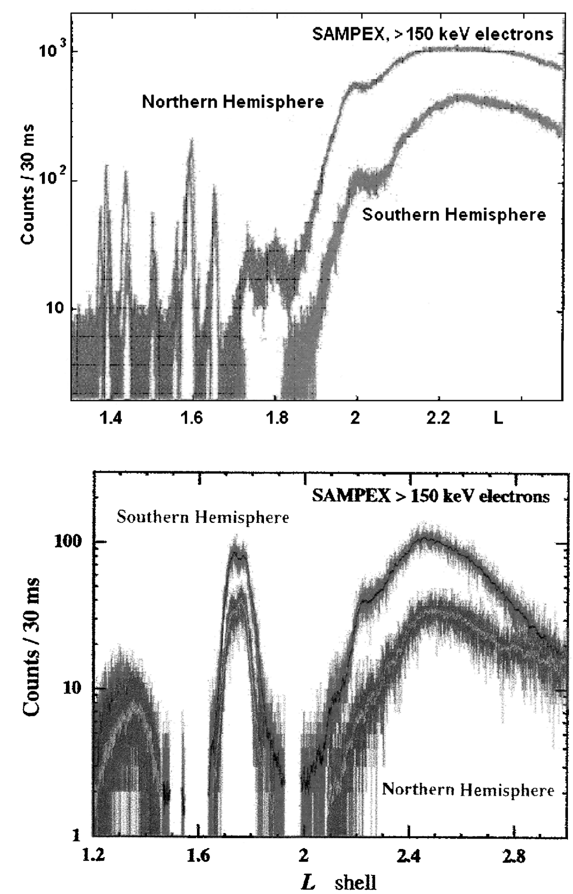

Fig. 4 South-to-north pass of SAMPEX.

experimental data at $L > 2$ and in the region of the South Atlantic anomaly, the position of electron flux precipitation at selected L values and the dependence of these zones on altitude (500, 700, 900, 1100, and 1300 km) are shown.

The value of electron energy is 30–500 keV. (Every section of the figure is plotted for the whole energy range.) The following is obvious from the figure:

1) Zones of electron flux registration under the inner radiation belt exist constantly in an altitude interval from 350 km (see preceding figure based on other satellite experiments) up to 1300 km.

2) Electrons are observed at $L = 1.2$–1.8 both in northern and in southern hemispheres.

3) The longitudinal size of the zones practically does not depend on altitude up to 1300 km, at higher altitudes the electron flux

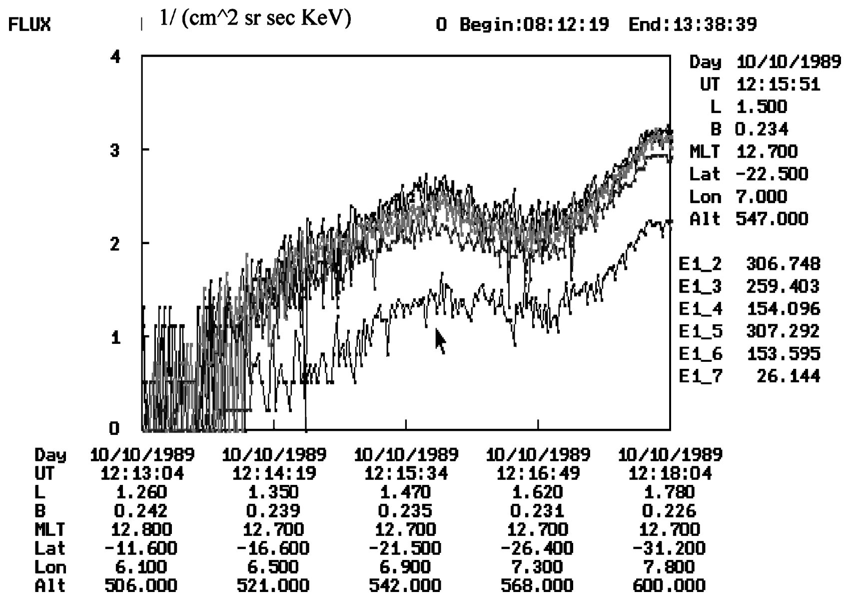

Fig. 5 Time history of the electron flux intensity at the ACTIVE satellite.

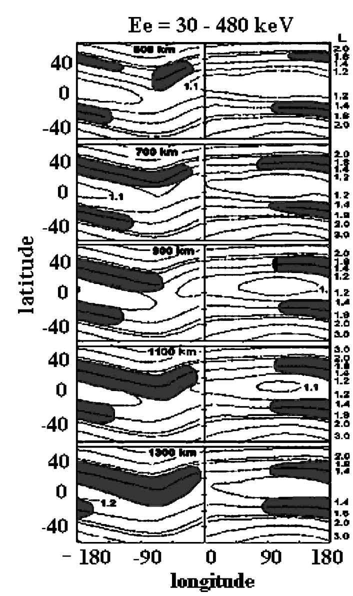

Fig. 6 Electron flux distribution at different altitudes.

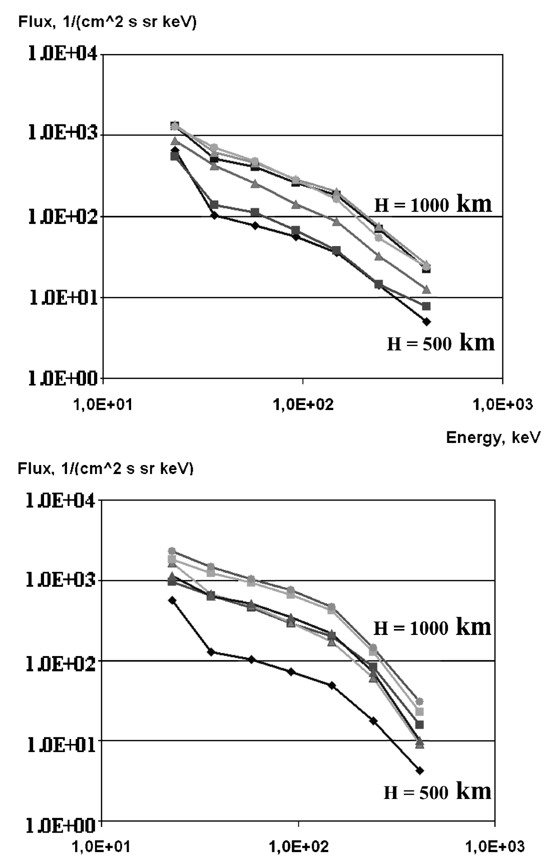

Fig. 7 Electron spectra at $L = 1.2$–1.5 (upper panel) and $L = 1.6$–1.9 lower panel) plotted for different altitudes from 500 to 1000 km with a step of 100 km.

becomes larger all over the latitude–longitude plane and it is difficult to allocate the selected formations.

Electron spectra at different altitudes from 500 to 1000 km in two L zones, $L = 1.2$–1.5 (upper panel) and $L = 1.6$–1.9 (bottom panel) are presented in Fig. 7. It is clearly seen that the electron flux value increases with the altitude (10 times more at 1000 than at 500 km). The results obtained in the ACTIVE satellite experiment are compared in Fig. 8 with other experimental data and with AE8 MIN and AE8 MAX models. Electron spectra obtained on board the MIR station (SPRUT-VI experiment) and the SAMPEX satellite and ACTIVE satellite experiments are presented. These satellites and the MIR station were launched on different orbits, so there are experimental data for a wide altitude range. SPRUT-VI data give the minimal value of electron flux as the data were obtained at 350-km altitude.[5] ACTIVE satellite data allow comparison of electron fluxes at different altitudes from 500 up to 100 km. At 1000 km altitude the electron flux has the value of AE8 model flux.

V. Absorbed Radiation Dose

In terms of these data, the observed radiation dose values were computed for the ACTIVE satellite orbit for two values of altitude (500 and 1000 km). The results of computation of the annual absorbed radiation dose in Si at different thicknesses (shown at long axis) of an infinite flat Al shield for electron fluxes for 500 km (bottom) and 1000 km altitude (top) are presented in Fig. 9. It is seen that contribution to absorbed dose of middle-latitude electron formations in the inner radiation belt at $L = 1.2$–1.9 increases with the altitude and it is important to take it into account.

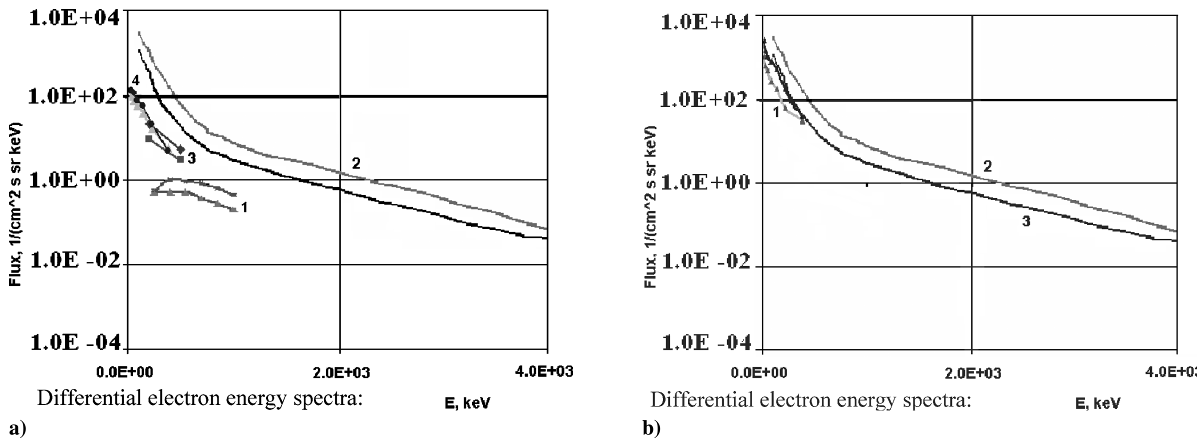

Fig. 8 Electron energy spectra compared with AE8MAX/MIN models: a) 1, SPRUT-VI data for $L = 1.2–1.4$ (bottom) and $L = 1.6–1.8$ (top) (altitude = 350 km); 2, AE8 MIN (top) and AE8 MAX (bottom) models data accordingly; 3, SAMPEX data for $L = 1.2–1.4$ (bottom) and $L = 1.6–1.8$ (top) (altitude = 600 km); and 4, ACTIVE data for $L = 1.2–1.4$ (bottom) and $L = 1.6–1.8$ (top) (altitude = 550 km); and b) 1, ACTIVE data for $L = 1.2–1.4$ (bottom) and $L = 1.6–1.8$ (top) (altitude = 1000 km); and 2 and 3, AE8 MIN and AE8 MAX model data accordingly.

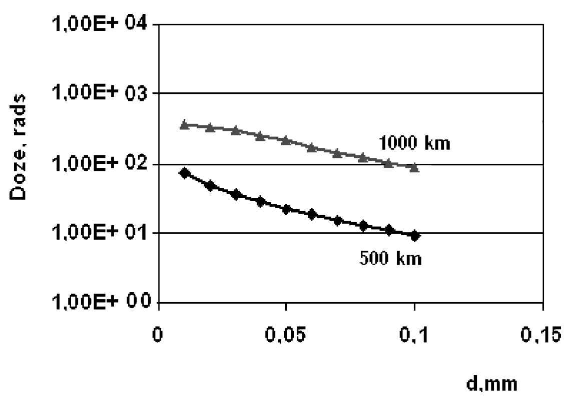

Fig. 9 Absorbed electron doses for various spectra of electron flux at 500 and 1000 km.

VI. Conclusions

Spacecraft were exposed to the impact of charged particles almost at low and middle latitudes (L-shell value from 1.2 to 1.8). The contribution of middle latitudes electron formation increases with the altitude and is 10 times greater at 1000 km than at 500 km. For a more correct estimate of the absorbed radiation dose value, the improved AE8 model for low energy values would be useful.

References

[1]Grachev, Y. A., Grigoryan, O. R., Novikov, L. S., and Tchurilo, I. V., "The Role of Proton and Electron 'Abnormal' Formation in Radiation Influence on Construction Elements of Spacecraft," *Proceedings of the ICPMSE-6. Protection of Materials and Structures from Space Environment*, edited by J. I. Kleiman and Z. Iskanderova, Kluwer Academic, Dordrecht, The Netherlands, 2003, pp. 123–130.

[2]Bashkirov, V. F., Denisov, Y. I., Gotseluk, Y. V., Kuznetsov, S. N., Myagkova, I. N., and Sinyakov, A. V., "Trapped and Quasi-Trapped Radiation Observed by CORONAS-I Satellite," *Radiation Measurements*, Vol. 30, No. 5, 1999, pp. 537–546.

[3]Grachev, E. A., Grigoryan, O. R., Klimov, S. I., Kudela, K., Petrov, A. N., Schwingenschuh, K., Sheveleva, V. N., and Stetiarova, J., "Altitude Distribution Analysis of Electron Fluxes at L = 1.2–1.8," *Advances in Space Research*, Vol. 36, No. 10, 2005, pp. 1992–1996.

[4]Blake, J. B., Inan, U. S., Walt, M., Bell, T. F., Bortnik, J., Chenette, D. L., and Christian, H. J., "Lightning-Induced Energetic Electron Flux Enhancements in the Drift Loss Cone," *Journal of Geophysical Research*, Vol. 106, No. A12, 2001, pp. 29,733–29,744.

[5]Biryukov, A., Grigoryan, O., Kuznetsov, S., Ryaboshapka, A., and Ryabukha, S., "Low-Energy Charged Particles at Near Equatorial Latitudes According to MIR Orbital Station Data," *Advances in Space Research*, Vol. 17, No. 10, 1996, pp. 189–192.

D. Edwards
Associate Editor